Original Article

Latin American Journal of Solids and Structures
www.lajss.org

1D analysis of laminated composite and sandwich plates using a new fifth-order plate theory

Abstract
In the present study, a new fifth-order shear and normal deformation theory (FOSNDT) is developed for the analysis of laminated composite and sandwich plates under cylindrical bending. The theory considered the effects of transverse shear and normal deformations. To account for the effect of transverse shear deformation, in-plane displacement uses polynomial shape function expanded up to fifth-order in-terms of the thickness coordinate. Transverse displacement uses derivative of shape function to account for the effect of transverse normal deformations. Therefore, the present theory involves six independent unknown variables. The theory satisfies traction free boundary conditions at top and bottom surfaces of the plate and does not require the shear correction factor. The principle of virtual work is used to obtain the variationally consistent governing differential equations and associated boundary conditions. Analytical solutions for simply supported boundary conditions are obtained using Navier's solution technique. Non-dimensional displacements and stresses obtained using the present theory are compared with existing exact elasticity solutions and lower and higher-order theories to prove the efficacy of the present theory. The comparison shows that the displacements and stresses predicted by the present theory are in good agreement with those obtained by using the exact solution.

Keywords
Fifth-order, shear deformation, normal deformation, laminated, sandwich, bending.

N. S. Naik [a*]
A. S. Sayyad [b]

[a] Research Scholar, Department of Civil Engineering, SRES's Sanjivani College of Engineering, Savitribai Phule Pune University, Kopargaon-423603, Maharashtra, India. E-mail: nitin_adi59@rediffmail.com

[b] Professor, Department of Civil Engineering, SRES's Sanjivani College of Engineering, Savitribai Phule Pune University, Kopargaon-423603, Maharashtra, India. E-mail: attu_sayyad@yahoo.co.in

*Corresponding author

http://dx.doi.org/10.1590/1679-78253973

Received: April 26, 2017
In Revised Form: September 23, 2017
Accepted: October 10, 2017
Available online: February 05, 2018

1 INTRODUCTION

The demand for high-strength, high-modulus and low density composite materials have generated an increased number of applications in many industries such as in aircraft, spacecraft, civil engineering, mechanical engineering, marine and many more.

The development of plate theory has a long history. Many well-known engineers, scientists, and mathematicians have made their contribution in the development of beam, plate and shell theories such as Jacob (II) Bernoulli, Leonard Euler, Joseph-Louis Lagrange Simeon Denis Poisson, Claude-Louis Navier and Gustav Robert Kirchhoff. The historical review of the development of beam, plate and shell theories is given in Timoshenko and Woinowsky-Krieger (1959), Todhunter and Pearson (1960) and Carrera et al. (2011).

Well-known exact elasticity solutions for one dimensional and two dimensional bending of laminated composite and sandwich plates are developed by Pagano (1969, 1970a, 1970b). These solutions serves as benchmark solutions for the comparison of results obtained by using analytical or numerical solutions based on approximate plate theories. Exact elasticity solutions are mathematically difficult and computationally more cumbersome. This led to the development of analytical and numerical solution based on approximate plate theories. The simplest plate theory, based on the displacement field, is the classical plate theory (CPT) developed by Kirchhoff (1850) in the nineteenth century. But, since shear deformation effect is neglected by the CPT it cannot be applied for the analysis of thick plates where shear deformation effect is more pronounced. Mindlin (1951) has considered the effect of transverse shear deformation for the first time in his first-order shear deformation theory (FSDT). The FSDT suffers from the drawback of constant shear strain condition through the thickness of the plate. Also it requires shear correction factor to properly account the strain energy due to shear deformation. These limitations of CPT and FSDT led to the development of higher-order shear deformation theories. The development of various higher-order plate theories and the solution techniques are recently reviewed by Sayyad and Ghugal (2015a).

Reddy (1984) has developed a simple higher-order shear deformation theory (HSDT) for laminated composite beams and plates. This HSDT is further used by many researchers for the solution of various solid mechanics problems. Kant and Kommineni (1994) have established a refined higher-order shear deformation theory for linear and geometrically non-linear behavior of fiber reinforced angle ply laminated composite and sandwich plates based on finite element formulation using a Lagrangian approach. Soldatos and Watson (1997) and Shu and Soldatos (2000) developed the hyperbolic shear deformation theory for the cylindrical bending of cross-ply and angle-ply laminates.

Chakrabarti and Sheikh (2005) have developed a finite element model for the bending analysis of soft core sandwich plates. A study of global-local higher-order theories for laminated composite plates is performed by Zhen and Wanji (2007) by presenting the general formulas of n^{th} order global local higher-order theory. Fares and Elmarghany (2008) have presented a refined zig-zag nonlinear FSDT of laminated composite plates using the Galerkin method. Ferreira et al. (2011) applied the Carrera's unified formulation (CUF) for predicting the free vibration, static deformation and buckling behavior of thin and thick cross-ply laminated plates. Carrera and Zappino (2016) proposed several models based on 1D, 2D and 3D kinematics for free vibrations of shell structures using Lagrange polynomials. Pagani et al. (2016) have developed refined computational model based on layer-wise approach using CUF for the analysis of laminated structures. Sarangan and Singh (2016) have presented higher-order closed form solutions for the static, buckling and free vibration analysis of laminated composite and sandwich plates based on new shear deformation theories using Navier's closed form solution technique. Kant and Shiyekar (2008) obtained Navier type closed form solutions for the cylindrical bending of piezoelectric laminates subjected to electro-mechanical loading using higher-order shear and normal deformation theory. Sayyad and Ghugal (2015b) applied a n^{th} order shear deformation theory for the cylindrical bending of composite laminates. Ghugal and Sayyad (2011) presented trigonometric shear and normal deformation theory for the free vibration of thick isotropic square and rectangular plate which was further extended by Sayyad and Ghugal (2016) for the cylindrical bending of multilayered composite laminates and sandwiches. A critical review of literature on bending, buckling and free vibration analysis of shear deformable isotropic, laminated composite and sandwich beams based on equivalent single layer theories, layerwise theories, zig-zag theories and exact elasticity solution has recently been presented by Sayyad and Ghugal (2017a). Sayyad and Ghugal (2017b) have also developed a displacement based unified shear deformation theory for the analysis of shear deformable advanced composite beams and plates.

1.1 The plate under consideration for the present study

A cross-ply laminated composite plate made of orthotropic fibrous composite material having length *'a'* and width *'b'* in the in the x and y directions respectively is considered as shown in Figure 1. The y direction of the plate is assumed to be infinitely long compared to other two dimensions, therefore, strains in the y direction are assumed to be zero ($\varepsilon_y = \gamma_{yz} = 0$). The thickness of the plate is measured in z-direction and at $z=0$, the mid plane of the plate is located. The plate under consideration consists of N number of layers bonded together. The plate is carrying an out of plane load $q(x)$, acting on its top surface. i.e. $\left(z = -h/2\right)$.

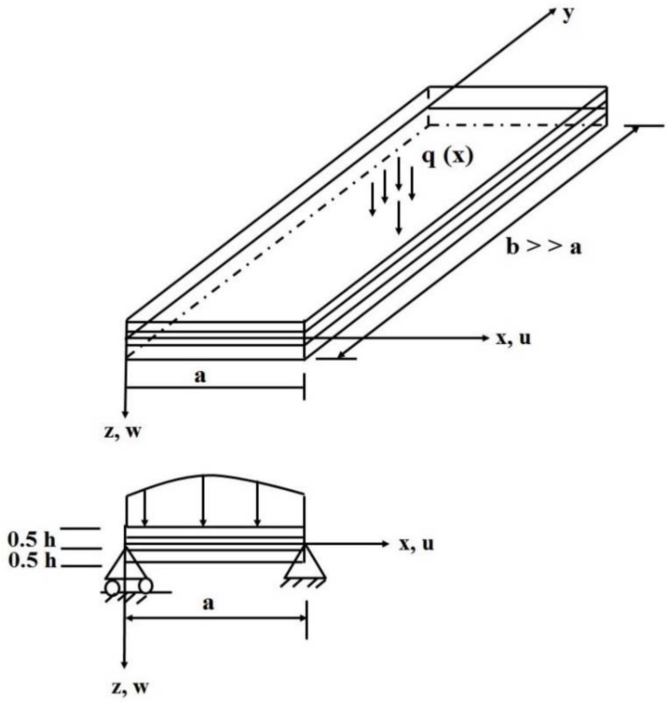

Figure 1: Geometry and co-ordinate system of the layered plate deform in cylindrical bending

2 FIFTH-ORDER SHEAR AND NORMAL DEFORMATION THEORY

Through-thickness distributions of transverse shear and normal stresses for composite laminates are important for delamination type failure. Therefore, it is essential to understand and calculate transverse shear and normal stress through the thickness of the plate accurately (Carrera 2005). However, in a whole variety of higher-order plate theories existing in the literature very few researchers have considered the effect of transverse normal stress for developing refined plate theory in view of minimizing the number of unknown variables. In the well-known theory of Reddy (1984), thickness coordinate is expanded up to third-order in the in-plane displacement field and the effect of transverse normal deformation is neglected.

The present theory is built upon classical plate theory having following important features.

1) The present theory considers the effects of transverse shear and normal deformations $\left(\varepsilon_z \neq 0\right)$.

2) The axial displacement in the x direction consists of extension, bending and shear components. The extension $\left(u_0\right)$ and bending $\left(u_b\right)$ components are analogues to the classical plate theory whereas the shear component $\left(u_s\right)$ contains polynomial shape function expanded up to fifth-order in terms of the thickness coordinate (*z/h*). Hence the theory is designated as the fifth-order shear and normal deformation theory (FOSNDT).

$$u = u_0 + u_b + u_s \tag{1}$$

Where

$$u_b = -z\frac{dw_0}{dx} \text{ and } u_s = \left[z - \frac{4z^3}{3h^2}\right]\phi_x + \left[z - \frac{16z^5}{5h^4}\right]\psi_x \tag{2}$$

3) The transverse displacement w in z- direction is assumed to be a function of x and z coordinates to include the effect of transverse normal deformations $\left(\varepsilon_z \neq 0\right)$.

$$w = w_0 + \left(1 - \frac{4z^2}{h^2}\right)\phi_z + \left(1 - \frac{16z^4}{h^4}\right)\psi_z \tag{3}$$

4) The theory enforces the parabolic variation of the transverse shear stress across the thickness of the plate. Thus, the theory obviates the need of the shear correction factor.
5) The body forces are not considered in the analysis.

2.1 Kinematics of the present theory

Based on the aforementioned assumptions and features, the displacement field of the present theory (FOSNPT) can be expressed as

$$u(x,z)=u_0(x)-z\frac{dw_0}{dx}+\left[z-\frac{4z^3}{3h^2}\right]\phi_x(x)+\left[z-\frac{16z^5}{5h^4}\right]\psi_x(x)$$
$$w(x,z)=w_0(x)+\left(1-\frac{4z^2}{h^2}\right)\phi_z(x)+\left(1-\frac{16z^4}{h^4}\right)\psi_z(x) \tag{4}$$

where u and w are the x and z-directional displacements of any point on the plate, u_0 and w_0 are the in-plane displacements of mid-plane in x and z-directions respectively; ϕ_x and ψ_x are rotations of the normal to the middle plane about y axis which account the effect of transverse shear deformation. ϕ_z and ψ_z represent higher-order transverse cross-sectional deformation modes i.e. effect of transverse normal deformations. The non-zero strain components associated with the present displacement field are obtained by using the linear theory of elasticity.

$$\varepsilon_x=\frac{\partial u}{\partial x}=\frac{du_0}{dx}-z\frac{d^2w_0}{dx^2}+\left(z-\frac{4z^3}{3h^2}\right)\frac{d\phi_x}{dx}+\left(z-\frac{16z^5}{5h^4}\right)\frac{d\psi_x}{dx}$$
$$\varepsilon_z=\frac{\partial w}{\partial z}=\left(-\frac{8z}{h^2}\right)\phi_z+\left(-\frac{64z^3}{h^4}\right)\psi_z \tag{5}$$
$$\gamma_{xz}=\frac{\partial u}{\partial z}+\frac{\partial w}{\partial x}=\left(\phi_x+\frac{d\phi_z}{dx}\right)\left(1-\frac{4z^2}{h^2}\right)+\left(\psi_x+\frac{d\psi_z}{dx}\right)\left(1-\frac{16z^4}{h^4}\right)$$

2.2 Constitutive Equations

The constitutive equations for the k^{th} lamina are given by

$$\begin{Bmatrix}\sigma_x\\ \sigma_z\\ \tau_{xz}\end{Bmatrix}^k=\begin{bmatrix}Q_{11} & Q_{13} & 0\\ Q_{13} & Q_{33} & 0\\ 0 & 0 & Q_{55}\end{bmatrix}^k\begin{Bmatrix}\varepsilon_x\\ \varepsilon_z\\ \gamma_{xz}\end{Bmatrix}^k \tag{6}$$

where Q_{ij} are the reduced elastic constants in x-z plane, σ_x is the normal stress along x-direction, σ_z is the stress acting along z-direction and τ_{xz} is shear stress along z-direction. The following relationship between the reduced elastic constants and the engineering elastic constants are used.

$$Q_{11}=\frac{E_1(1-\mu_{23}\mu_{32})}{(1-\mu_{12}\mu_{21}-\mu_{23}\mu_{32}-\mu_{31}\mu_{13}-2\mu_{12}\mu_{23}\mu_{31})},$$
$$Q_{13}=\frac{E_1(\mu_{31}+\mu_{21}\mu_{32})}{(1-\mu_{12}\mu_{21}-\mu_{23}\mu_{32}-\mu_{31}\mu_{13}-2\mu_{12}\mu_{23}\mu_{31})}, \tag{7}$$
$$Q_{33}=\frac{E_3(1-\mu_{12}\mu_{21})}{(1-\mu_{12}\mu_{21}-\mu_{23}\mu_{32}-\mu_{31}\mu_{13}-2\mu_{12}\mu_{23}\mu_{31})},$$
$$Q_{55}=G_{13}$$

where E_1, E_3 are Young's moduli, G_{13} is the shear modulus and $\mu_{12}, \mu_{21}, \mu_{13}, \mu_{31}, \mu_{23}, \mu_{32}$ are Poisson's ratios; the subscripts 1, 2, 3 correspond to *x, y, z* directions of Cartesian coordinate systems, respectively.

2.3 Governing Equations and Boundary Conditions

Variationally consistent governing differential equations and associated boundary conditions are derived by using the principle of virtual work. For the plate under consideration, the principle of virtual work takes the following form.

$$b\int_0^L \int_{-h/2}^{+h/2} \left(\sigma_x \delta\varepsilon_x + \sigma_z \delta\varepsilon_z + \tau_{xz}\delta\gamma_{xz}\right) dz\, dx - \int_0^L q\delta w\, dx = 0 \tag{8}$$

where δ is the virtual displacement i.e. infinitesimal change in the position coordinates of the points under consideration. $q(x)$ represents transverse load acting on the top surface of the plate. By substituting virtual strain from Eq. (5) into the Eq. (8) one can obtain

$$\begin{aligned}\int_0^L &\left(N_x \frac{d\delta u_0}{dx} - M_x^b \frac{d^2\delta w_0}{dx^2} + M_x^{s_1}\frac{d\delta\phi_x}{dx} + M_x^{s_2}\frac{d\delta\psi_x}{dx} + Q_z^{S_1}\delta\phi_z \right. \\ &\left. + Q_z^{S_2}\delta\psi_z + Q_{xz}^1\delta\phi_x + Q_{xz}^1\frac{d\delta\phi_z}{dx} + Q_{xz}^2\delta\psi_x + Q_{xz}^2\frac{d\delta\psi_z}{dx}\right) dx = \int_0^L q\delta w\, dx\end{aligned} \tag{9}$$

where N_x represents the axial force resultant; M_x^b, M_x^s represent bending moment and higher order moment resultants; Q_{xz}^1, Q_{xz}^2 represent shear force resultants due to shear deformation; and $Q_z^{s_1}, Q_z^{s_2}$ represent shear force resultants due to normal deformations.

$$\begin{aligned}
N_x &= \int_{-h/2}^{+h/2}\sigma_x dz = A_{11}\frac{du_0}{dx} - B_{11}\frac{d^2w_0}{dx^2} + C_{11}\frac{d\phi_x}{dx} + D_{11}\frac{d\psi_x}{dx} + I_{13}\phi_z + J_{13}\psi_z \\
M_x^b &= \int_{-h/2}^{+h/2}\sigma_x z dz = B_{11}\frac{du_0}{dx} - A_{s11}\frac{d^2w_0}{dx^2} + C_{s11}\frac{d\phi_x}{dx} + D_{s11}\frac{d\psi_x}{dx} + I_{s13}\phi_z + J_{s13}\psi_z \\
M_x^{s_1} &= \int_{-h/2}^{+h/2}\sigma_x f_1(z) dz = C_{11}\frac{du_0}{dx} - C_{s11}\frac{d^2w_0}{dx^2} + C_{ss111}\frac{d\phi_x}{dx} + C_{ss211}\frac{d\psi_x}{dx} + I_{ss113}\phi_z + J_{ss113}\psi_z \\
M_x^{s_2} &= \int_{-h/2}^{+h/2}\sigma_x f_2(z) dz = D_{11}\frac{du_0}{dx} - D_{s11}\frac{d^2w_0}{dx^2} + C_{ss211}\frac{d\phi_x}{dx} + D_{ss111}\frac{d\psi_x}{dx} + I_{ss213}\phi_z + J_{ss213}\psi_z \\
Q_{xz}^1 &= \int_{-h/2}^{+h/2}\tau_{xz} f_1^{'}(z) dz = C_{sss155}\phi_x + C_{sss155}\frac{d\phi_z}{dx} + C_{sss255}\psi_x + C_{sss255}\frac{d\psi_z}{dx} \\
Q_{xz}^2 &= \int_{-h/2}^{+h/2}\tau_{xz} f_2^{'}(z) dz = C_{sss255}\phi_x + C_{sss255}\frac{d\phi_z}{dx} + D_{sss155}\psi_x + D_{sss155}\frac{d\psi_z}{dx} \\
Q_z^{S_1} &= \int_{-h/2}^{+h/2}\sigma_z f_1^{''}(z) dz = I_{13}\frac{du_0}{dx} - I_{s13}\frac{d^2w_0}{dx^2} + I_{ss113}\frac{d\phi_x}{dx} + I_{ss213}\frac{d\psi_x}{dx} + I_{sss133}\phi_z + I_{sss233}\psi_z \\
Q_z^{S_2} &= \int_{-h/2}^{+h/2}\sigma_z f_2^{''}(z) dz = J_{13}\frac{du_0}{dx} - J_{s13}\frac{d^2w_0}{dx^2} + J_{ss113}\frac{d\phi_x}{dx} + J_{ss213}\frac{d\psi_x}{dx} + I_{sss233}\phi_z + J_{sss133}\psi_z
\end{aligned} \tag{10}$$

where

$$f_1(z)=\left[z-\frac{4z^3}{3h^2}\right],\ f_1^{'}(z)=\left[1-\frac{4z^2}{h^2}\right],\ f_1^{''}(z)=\left[\frac{-8z}{h^2}\right],$$
$$f_2(z)=\left[z-\frac{16z^5}{5h^4}\right],\ f_2^{'}(z)=\left[1-\frac{16z^4}{h^4}\right],\ f_2^{''}(z)=\left[\frac{-64z^3}{h^4}\right] \tag{11}$$

The governing equations can be derived from Eq. (9) by integrating the displacement variables by parts and setting the coefficients of $\delta u_0, \delta w_0, \delta\phi_x, \delta\psi_x, \delta\phi_z$ and $\delta\psi_z$ to zero separately, and the following equations can be obtained:

$$\delta u_0:\ \frac{dN_x}{dx}=A_{11}\frac{d^2u_0}{dx^2}-B_{11}\frac{d^3w_0}{dx^3}+C_{11}\frac{d^2\phi_x}{dx^2}+D_{11}\frac{d^2\psi_x}{dx^2}+I_{13}\frac{d\phi_z}{dx}+J_{13}\frac{d\psi_z}{dx}=0 \tag{12}$$

$$\delta w_0:\ \frac{d^2M_x^b}{dx^2}+q=B_{11}\frac{d^3u_0}{dx^3}-A_{s11}\frac{d^4w_0}{dx^4}+C_{s11}\frac{d^3\phi_x}{dx^3}+D_{s11}\frac{d^3\psi_x}{dx^3}+I_{s13}\frac{d^2\phi_z}{dx^2}+J_{s13}\frac{d^2\psi_x}{dx^2}+q=0 \tag{13}$$

$$\begin{aligned}\delta\phi_x:\ \frac{dM_x^{S_1}}{dx}-Q_{xz}^1&=C_{11}\frac{d^2u_0}{dx^2}-C_{s11}\frac{d^3w_0}{dx^3}+C_{ss111}\frac{d^2\phi_x}{dx^2}+C_{ss211}\frac{d^2\psi_x}{dx^2}+I_{ss113}\frac{d\phi_z}{dx}\\&+J_{ss113}\frac{d\psi_z}{dx}-C_{sss155}\phi_x-C_{sss155}\frac{d\phi_z}{dx}-C_{sss255}\psi_x-C_{sss255}\frac{d\psi_z}{dx}=0\end{aligned} \tag{14}$$

$$\begin{aligned}\delta\psi_x:\ \frac{dM_x^{S_2}}{dx}-Q_{xz}^2&=D_{11}\frac{d^2u_0}{dx^2}-D_{s11}\frac{d^3w_0}{dx^3}+C_{ss211}\frac{d^2\phi_x}{dx^2}+D_{ss111}\frac{d^2\psi_x}{dx^2}+I_{ss213}\frac{d\phi_z}{dx}+\\&J_{ss213}\frac{d\psi_z}{dx}-C_{sss255}\phi_x-C_{sss255}\frac{d\phi_z}{dx}-D_{sss155}\psi_x-D_{sss155}\frac{d\psi_z}{dx}=0,\end{aligned} \tag{15}$$

$$\begin{aligned}\delta\phi_z:\frac{dQ_{xz}^1}{dx}-Q_z^{s_1}&=C_{sss155}\frac{d\phi_x}{dx}+C_{sss155}\frac{d^2\phi_z}{dx^2}+C_{sss255}\frac{d\psi_x}{dx}+C_{sss255}\frac{d^2\psi_z}{dx^2}-I_{13}\frac{du_0}{dx}+\\&I_{s13}\frac{d^2w_0}{dx^2}-I_{ss113}\frac{d\phi_x}{dx}-I_{ss213}\frac{d\psi_x}{dx}-I_{sss133}\phi_z-I_{sss233}\psi_z=0\end{aligned} \tag{16}$$

$$\begin{aligned}\delta\psi_z:\frac{dQ_{xz}^2}{dx^2}-Q_z^{s_2}&=C_{sss255}\frac{d\phi_x}{dx}+C_{sss255}\frac{d^2\phi_z}{dx^2}+D_{sss155}\frac{d\psi_x}{dx}+D_{sss155}\frac{d^2\psi_z}{dx^2}-J_{13}\frac{du_0}{dx}+\\&J_{s13}\frac{d^2w_0}{dx^2}-J_{ss113}\frac{d\phi_x}{dx}-J_{ss213}\frac{d\psi_x}{dx}-I_{sss233}\phi_z-J_{sss133}\psi_z=0\end{aligned} \tag{17}$$

where the extension, bending, bending-extension, bending-twisting stiffnesses used in the equations (12) -(17) can be obtained as

$$\left(A_{ij}, B_{ij}, A_{sij}\right) = Q_{ij} \int_{-h/2}^{+h/2} \left(1, z, z^2\right) dz,$$

$$\left(C_{ij}, C_{sij}, C_{ss1ij}, C_{ss2ij}, I_{ss1ij}, J_{ss1ij}\right) = Q_{ij} \int_{-h/2}^{+h/2} f_1(z)\left[1, z, f_1(z), f_2(z), f_1''(z), f_2''(z)\right] dz,$$

$$\left(D_{ij}, D_{sij}, D_{ss1ij}, I_{ss2ij}, J_{ss2ij}\right) = Q_{ij} \int_{-h/2}^{+h/2} f_2(z)\left[1, z, f_2(z), f_1''(z), f_2''(z)\right] dz, \tag{18}$$

$$\left(C_{sss1ij,} C_{sss2ij}\right) = Q_{ij} \int_{-h/2}^{+h/2} f_1'(z)\left[f_1'(z), f_2'(z)\right] dz, \left(D_{sss1ij}\right) = Q_{ij} \int_{-h/2}^{+h/2} f_2'(z)\, f_2'(z) dz,$$

$$\left(I_{ij}, I_{sij}, I_{sss1ij}, I_{sss2ij}\right) = Q_{ij} \int_{-h/2}^{+h/2} f_1''(z)\left[1, z, f_1''(z), f_2''(z)\right] dz,$$

$$\left(J_{ij}, J_{sij}, J_{sss1ij}\right) = Q_{ij} \int_{-h/2}^{+h/2} f_2''(z)\left[1, z, f_2''(z)\right] dz$$

The boundary conditions along edges ($x = 0$, $x = a$) are of the following form:

$$N_x = 0 \text{ or } u_0 = 0; \quad M_x^b = 0 \text{ or } dw_0/dx = 0; \quad dM_x^b/dx = 0 \text{ or } w_0 = 0; \quad M_x^{s_1} = 0 \text{ or } \phi_x = 0$$
$$M_x^{s_2} = 0 \text{ or } \psi_x = 0; \quad Q_{xz}^1 = 0 \text{ or } \phi_z = 0; \quad Q_{xz}^2 = 0 \text{ or } \psi_z = 0 \tag{19}$$

2.4 Closed form solutions

For a simply supported laminated composite plate, the kinematic boundary conditions are given below:

$$w_0 = 0,\ N_x = 0,\ M_x^b = 0,\ M^{s_1} = 0,\ M^{s_2} = 0 \tag{20}$$

To determine the unknown displacement variables, the Navier's solution technique is implemented. To satisfy the aforementioned boundary conditions the displacements and rotations are assumed in Fourier trigonometric form

$$\left(u_0, \phi_x, \psi_x\right) = \sum_{m=1}^{\infty} \left(u_m, \phi_{xm}, \psi_{xm}\right) \cos\left(\frac{m\pi x}{a}\right)$$
$$\left(w_0, \phi_z, \psi_z\right) = \sum_{m=1}^{\infty} \left(w_m, \phi_{zm}, \psi_{zm}\right) \sin\left(\frac{m\pi x}{a}\right) \tag{21}$$

where $u_m, w_m, \phi_{xm}, \psi_{xm}, \phi_{zm}$ and ψ_{zm} are the unknowns to be determined. According to Navier's solution scheme, transverse load is also expanded in Fourier trigonometric form

$$q(x) = \sum_{m=1}^{\infty} q_m \sin\left(\frac{m\pi x}{a}\right) \tag{22}$$

where q_m is the coefficient of Fourier series expansion and m is the positive integer. For sinusoidal load, $q_m = q_0$ and m=1. Substitution of Eqs. (21) and (22) into governing equations (12) through (17) leads to the following form

$$\begin{bmatrix} K_{11} & K_{12} & K_{13} & K_{14} & K_{15} & K_{16} \\ & K_{22} & K_{23} & K_{24} & K_{25} & K_{26} \\ & & K_{33} & K_{34} & K_{35} & K_{36} \\ & & & K_{44} & K_{45} & K_{46} \\ & \text{symmetric} & & & K_{55} & K_{56} \\ & & & & & K_{66} \end{bmatrix} \begin{Bmatrix} u_m \\ w_m \\ \phi_{xm} \\ \psi_{xm} \\ \phi_{zm} \\ \psi_{zm} \end{Bmatrix} = \begin{Bmatrix} 0 \\ q_m \\ 0 \\ 0 \\ 0 \\ 0 \end{Bmatrix} \tag{23}$$

where $[K_{ij}]$ are the elements of stiffness matrix

$$K_{11} = -A_{11}\left(\frac{m^2\pi^2}{a^2}\right),\ K_{12} = B_{11}\left(\frac{m^3\pi^3}{a^3}\right),\ K_{13} = -C_{11}\left(\frac{m^2\pi^2}{a^2}\right),\ K_{14} = -D_{11}\left(\frac{m^2\pi^2}{a^2}\right);\ K_{15} = I_{13}\left(\frac{m\pi}{a}\right),$$

$$K_{16} = J_{13}\left(\frac{m\pi}{a}\right), K_{22} = -A_{s11}\left(\frac{m^4\pi^4}{a^4}\right), K_{23} = C_{s11}\left(\frac{m^3\pi^3}{a^3}\right), K_{24} = D_{s11}\left(\frac{m^3\pi^3}{a^3}\right), K_{25} = -I_{s13}\left(\frac{m^2\pi^2}{a^2}\right),$$

$$K_{26} = -J_{s13}\left(\frac{m^2\pi^2}{a^2}\right),\ K_{33} = -C_{ss111}\left(\frac{m^2\pi^2}{a^2}\right) - C_{sss155},\ K_{34} = -\left[C_{ss211}\left(\frac{m^2\pi^2}{a^2}\right) + C_{sss255}\right], \tag{24}$$

$$K_{35} = I_{ss113}\left(\frac{m\pi}{a}\right) - C_{sss155}\left(\frac{m\pi}{a}\right), K_{36} = J_{ss113}\left(\frac{m\pi}{a}\right) - C_{sss255}\left(\frac{m\pi}{a}\right), K_{45} = I_{ss213}\left(\frac{m\pi}{a}\right) - C_{sss255}\left(\frac{m\pi}{a}\right),$$

$$K_{46} = J_{ss213}\left(\frac{m\pi}{a}\right) - D_{sss155}\left(\frac{m\pi}{a}\right), K_{56} = -C_{sss255}\left(\frac{m^2\pi^2}{a^2}\right) - I_{sss233}, K_{66} = -D_{sss155}\left(\frac{m^2\pi^2}{a^2}\right) - J_{sss133}$$

After knowing the values of unknown displacement variables $u_0, w_0, \phi_x, \psi_x, \phi_z$ and ψ_z from Eq. (23), one can obtain all the displacements and stress components within the laminated composite plate using equations (4) through (6).

2.5 Estimation of transverse shear stress and normal stress

Through-thickness distributions of transverse shear and normal stresses for composite laminates are important for delamination type failure. The evaluation of transverse shear stresses from the constitutive relations leads to discontinuity at the inter face of two adjacent layers of a laminate and thus violates the equilibrium conditions. Thus, elasticity equilibrium equation neglecting the body force is used to derive expression for the transverse stress in the k^{th} lamina of composite laminate.

$$\tau_{xz}^k = -\int_{h_k}^{h_{k+1}} \frac{\partial \sigma_x^k}{\partial x} dz + C \tag{25}$$

From equation (25) the transverse stress (τ_{xz}) can be evaluated through integration with respect to the laminate thickness coordinate (*z*). The in-plane stress (σ_x) obtained by using equation (4) is substituted in equation (25). The constants of integrations (*C*) can be determined by substituting the boundary conditions. It is expected that this procedure will produce an accurate transverse shear stresses.

3.0 NUMERICAL RESULTS AND DISCUSSION

Aluminum alloy and fibrous composite materials are being used increasingly for numerous space applications.

3.1 Aluminum alloy: Aluminum is one of the most widely used metals in modern aircraft construction. It is vital to the aviation industry because of its high strength to weight ratio and its comparative ease of fabrication. The outstanding characteristic of aluminum is its light weight. Aluminum melts at the comparatively low temperature of 1250^{0}F. It is nonmagnetic and is an excellent conductor. Following material properties (Aluminum 3003-H14) are used for numerical study.

Material 1 (Krishna Murty, 1984): $E_1 = E_2 = E_3 = E = 69\ GPa$ and $G_{12} = G_{13} = G_{23} = G = 26\ GPa$

3.2 Fibrous composite materials: Engineers are interested in these materials because of their favorable mechanical characteristic of high strength/high stiffness to weight ratio and potential for zero or near-zero coefficient of thermal expansion. The use of high modulus Graphite-Epoxy composite parts for space applications is already well established. Using Graphite-Epoxy parts for space vehicles and structures has many advantages including: 1) Critical weight savings 2) Improved control of thermal distortions 3) Increased structural stiffness. Following properties of Graphite-Epoxy composite material are used for the numerical study.

Material 2 (Pagano, 1969): $E_1 = 172.5\ GPa$, $E_2 = E_3 = 6.9\ GPa$, $G_{12} = G_{13} = 3.45\ GPa$, $G_{23} = 1.38\ GPa$, $\mu_{12} = \mu_{13} = \mu_{23} = 0.25$

Material 3 (Kant and Swaminathan, 2000): $E_1 = 131.1\ GPa$, $E_2 = E_3 = 6.9\ GPa$, $G_{12} = G_{13} = 3.588\ GPa$, $G_{23} = 3.088\ GPa$, $\mu_{12} = \mu_{13} = 0.32$, $\mu_{23} = 0.49$

Material 4 (Kapuria et al., 2004): $E_1 = 0.2208\ MPa$, $E_2 = 0.2001\ MPa$, $E_3 = 2760\ MPa$, $G_{12} = 16.56\ MPa$, $G_{23} = 455.4\ MPa$, $G_{31} = 545.1\ MPa$, $\mu_{12} = 0.99$, $\mu_{13} = \mu_{23} = 0.00003$

For the validity of the present theory, following examples are solved for the numerical study.

a) Cylindrical bending of two-layer ($0^0/90^0$) antisymmetric cross-ply laminated composite plates. (Figure 2a)
b) Cylindrical bending of three-layer ($0^0/90^0/0^0$) symmetric cross-ply laminated composite plates. (Figure 2b)
c) Cylindrical bending of three-layer (0^0/*core*/0^0) symmetric sandwich plates. (Figure2C)

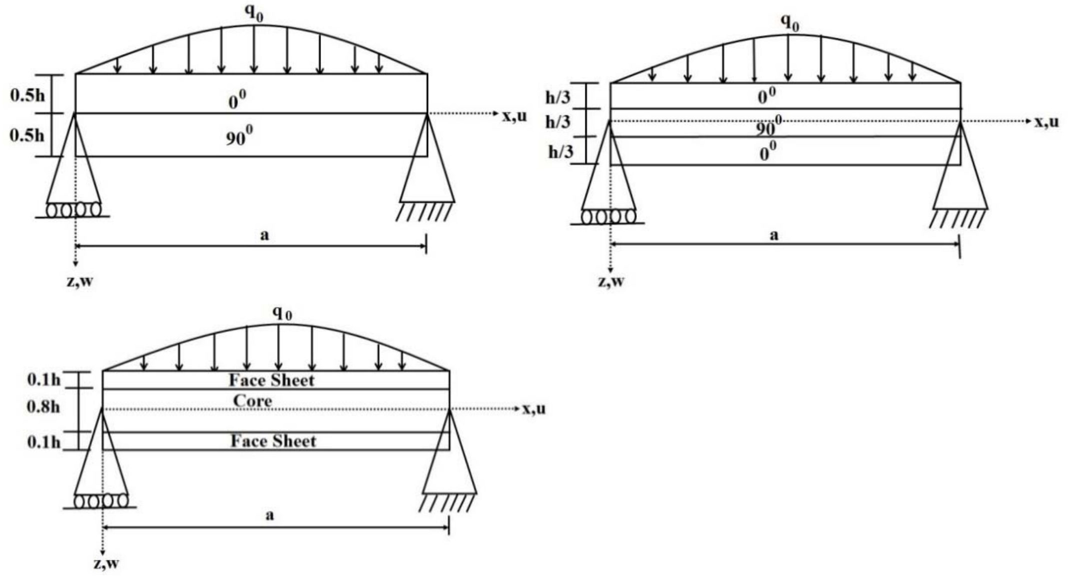

Figure 2: *Simply supported laminated plates subjected to sinusoidal load*

Displacements and stresses for laminated composite and sandwich plates under cylindrical bending obtained by using the present theory (FOSNDT) are presented in Tables 1-4 and compared with the those obtained by using the classical plate theory (CPT), FSDT of Mindlin (1951), HSDT of Reddy (1984), sinusoidal shear and normal deformation theory of Sayyad and Ghugal (2016). Exact elasticity solution developed by Pagano (1969) is considered as a benchmark solution for comparison. The displacements and stresses are calculated at typical important locations and presented in the following non-dimensional form.

$$\bar{u}\left(0,-\frac{h}{2}\right)=\frac{bE_3u}{q_0h},\ \bar{w}\left(\frac{a}{2},0\right)=\frac{100E_3wh^3b}{q_0a^4},\ \bar{\sigma}_x\left(\frac{a}{2},-\frac{h}{2}\right)=\frac{b\sigma_x}{q_0},\ \bar{\tau}_{xz}\left(0,0\right)=\frac{b\tau_{xz}}{q_0} \qquad (26)$$

The through-the-thickness profiles for in-plane displacement ($\bar{u}$), in-plane normal stress ($\bar{\sigma}_x$) and transverse shear stress ($\bar{\tau}_{xz}$) for laminated and sandwich plates subjected to a sinusoidal load are plotted in Figures 3 through 14.

High-strength aluminum alloy is an important airframe material since 1920s. Therefore, the present theory is tested for the plate made of aluminum alloy (material 1). Comparison of non-dimensional displacements and stresses of aluminum alloy plate subjected to sinusoidal load are tabulated in Table 1. For the comparison purpose, numerical results by using HSDT of Reddy (1984), FSDT of Mindlin (1951) and CPT are obtained. The numerical results are presented for thick ($a/h = 4$), moderately thick ($a/h = 10$) and thin plates ($a/h = 100$). From Table 1, it is pointed out that numerical results obtained by using the present theory and HSDT of Reddy (1984) are in excellent agreement with each other whereas FSDT and CPT underestimate the displacements and stresses due to neglect of shear and normal deformations.

The comparison of non-dimensional displacements and stresses for the two-layer ($0^0/90^0$) laminated composite plates is shown in Table 2. The plate is subjected to a sinusoidal load (Figure 2*a*) and made up of orthotropic material 2. Both the layers are of equal thickness i.e. $h/2$. Through-the-thickness distributions of in-plane displacement and stresses are plotted in Figures 3-5 and variation of transverse displacement with respect to a/h ratio is plotted in Figure 6. Exact elasticity solutions presented by Pagano (1969) are taken as basis for the comparison of numerical results obtained by using the present theory (FOSNDT), HSDT of Reddy (1984), SSNPT of Sayyad and Ghugal (2016), FSDT of Mindlin (1951) and CPT. HSDT, FSDT and CPT do not consider the effect of transverse normal deformation ($\varepsilon_z=0$) whereas the present theory and SSNPT considers the effect of transverse normal deformation ($\varepsilon_z\neq0$). It can be observed from Table 2 that the present theory shows considerable improvement in the in-plane displacement and stresses compared to those obtained by using HSDT and SSNPT. The percentage error predicted using the present theory is less in many cases as compared to HSDT, SSNPT, FSDT and CPT. This is in fact due to inclusion of fifth order term in-terms of the thickness coordinate in the displacement field. Figures 4 and 5 shows stresses are always maximum in 0^0 layer and minimum in 90^0 layers. The transverse shear stress ($\bar{\tau}_{xz}$) which is an important indicator to the onset of delamination are obtained using equations of equilibrium to ascertain the continuity at the layer interface. Through-the-thickness distribution of transverse displacement is not uniform when itis obtained using the present theory and SSNPT whereas it is uniform when obtained by using HSDT, FSDT and CPT.

Table 3 compares numerical values of non-dimensional displacements and stresses obtained by using the present theory and other higher-order theories for three-layer ($0^0/90^0/0^0$) symmetric laminated composite plate subjected to a sinusoidal load (see Figure 2*b*). The plate is made of material 2 and overall thickness is equally distributed among all the layers i.e. $h/3$. The examination of Table 3 reveals that present results are in excellent agreement with those obtained by using the exact elasticity solution of Pagano (1969). In this problem also considerable improvement in the results is observed due to refinement of the polynomial shape function. Large percentage error is observed when these quantities are obtained by using FSDT and CPT due to neglect of shear and normal deformations. Through-the-thickness distributions of in-plane displacement and stresses are plotted in Figures 7-9. Variation of transverse displacement with respect to *a/h* ratios is plotted in Figure 10.

Table 4 compares the numerical values of non-dimensional displacement and stresses of three-layer (0^0/*core*/90^0) symmetric sandwich plate subjected to a sinusoidal load (see Figure 2c). Thickness of top and bottom face sheets is $0.1h$ each whereas thickness of middle soft core is $0.8h$. Face sheets of the plate are made of a fibrous composite material 3 whereas the core is made of material 4. For the sandwich plates in cylindrical bending, the exact elasticity solution is not available in the literature; hence present results are compared with published results. Present results are in good agreement with the HSDT of Reddy (1984) and SSNPT of Sayyad and Ghugal (2016). Figure 10 shows variation of transverse displacement with respect to aspect ratio for the three-layer ($0^0/90^0/0^0$) symmetric laminated composite plate subjected to sinusoidal load. Figures 11-13 plots the through-the-thickness distributions of in-plane displacement, in-plane normal stress and transverse shear stress. The examination of Figure 12 reveals that the in-plane normal stress developed in the middle core is very small compared to that in top and bottom face sheets. This is in fact due to core material is soft compared to material of face sheets. The transverse shear stress is obtained using equations of equilibrium of the theory of elasticity to ascertain the stress continuity at the layer interface. Variation of transverse displacement with respect to *a/h* ratios is plotted in Figure 14.

Table 1. *Comparison of In-Plane Displacement, Transverse Displacement, In-Plane Normal Stress and Transverse Shear Stress for Aluminum Alloy Plate Subjected to Sinusoidal Load under Cylindrical Bending*

a/h	Theory	$\bar{u}^{max}$	$\bar{w}^{max}$	$\bar{\sigma}_x^{max}$	$\bar{\tau}_{xz}^{max}$
4	FOSNDT	11.165800	12.8280	10.0468	1.8964
	HSDT	11.398300	13.0150	10.0233	1.8953
	FSDT	11.061100	13.0194	9.72680	1.9099
	CPT	11.061100	11.0577	9.72680	1.9099
10	FOSNDT	173.23530	11.3061	61.2064	4.7708
	HSDT	173.67450	11.3253	61.0897	4.7688
	FSDT	172.82960	11.3253	60.7928	4.7746
	CPT	172.83010	11.0577	60.7927	4.7746
100	FOSNDT	173010.00	11.0169	6091.10	47.763
	HSDT	172858.81	11.0072	6080.28	47.751
	FSDT	172793.18	11.0036	6079.82	47.736
	CPT	172830.12	11.0577	6079.27	47.746

FOSNDT: Present, HSDT: Reddy (1984), FSDT: Mindlin (1951), CPT: Kirchhoff (1850)

Table 2. *Comparison of In-Plane Displacement, Transverse Displacement, In-Plane Normal Stress and Transverse Shear Stress for Two-Layer ($0^0/90^0$) Antisymmetric Laminated Composite Plate Subjected to Sinusoidal Load under Cylindrical Bending.*

a/h	ε_z	Model	$\bar{u}^{max}$	% Error	$\bar{w}^{max}$	% Error	$\bar{\sigma}_x^{max}$	% Error	$\bar{\tau}_{xz}^{max}$	% Error
4	≠0	FOSNDT	1.6721	-7.877	4.5159	-4.351	333.231	-10.663	2.9531	-9.3740
	≠0	SSNPT	1.7155	-10.67	4.3904	-1.451	333.855	-12.740	2.9900	-10.740
	0	HSDT	1.7071	10.13	4.4444	-2.698	333.606	-10.829	2.9770	-10.259
	0	FSDT	1.4176	8.541	4.7900	-10.68	227.905	7.0731	2.9468	-9.1400
	0	CPT	1.4176	8.541	2.6188	39.48	227.905	7.0731	2.9468	-9.1400
	≠0	Elasticity	1.5500	0.000	4.3276	0.000	330.029	0.000	2.7000	0.0000
10	≠0	FOSNDT	22.326	4.680	2.8766	2.715	1176.72	-0.982	7.2910	0.1232
	≠0	SSNPT	22.892	2.267	2.9066	1.701	1180.66	-3.234	7.3879	-1.204
	0	HSDT	22.886	2.292	2.9159	1.386	1180.20	-2.971	7.3780	-1.068
	0	FSDT	22.150	5.434	2.9662	-0.31	1174.40	0.342	7.3670	-0.917
	0	CPT	22.150	5.434	2.6188	11.43	1174.40	0.342	7.3670	-0.917
	≠0	Elasticity	23.423	0.000	2.9569	0.000	1175.00	0.000	7.3000	0.0000

FOSNDT: Present, SSNPT: Sayyad and Ghugal (2016), HSDT: Reddy (1984), FSDT: Mindlin (1951), CPT: Kirchhoff (1850), Elasticity: Pagano (1969)

Table 3. *Comparison of In-Plane Displacement, Transverse Displacement, In-Plane Normal Stress and Transverse Shear Stress for Three-Layer ($0^0/90^0/0^0$) Symmetric Laminated Composite Plate Subjected to Sinusoidal Load under Cylindrical Bending*

a/h	ε_z	Model	$\bar{u}^{max}$	% Error	$\bar{w}^{max}$	% Error	$\bar{\sigma}_x^{max}$	% Error	$\bar{\tau}_{xz}^{max}$	% Error
4	≠0	FOSNDT	0.9544	-0.463	2.7794	3.727	19.013	-5.92	1.5241	-6.580
	≠0	SSNPT	0.8885	6.473	2.7342	5.292	17.575	2.087	1.5278	-6.839
	0	HSDT	0.8640	9.052	2.6985	6.529	17.006	5.259	1.5565	-8.840
	0	FSDT	0.5124	46.06	2.4094	16.54	10.085	43.81	1.7690	-23.70
	0	CPT	0.5124	46.06	0.5097	82.34	10.085	43.81	1.7690	-23.70
	≠0	Elasticity	0.9500	0.000	2.8870	0.000	17.950	0.000	1.4300	0.0000
10	≠0	FOSNDT	9.3314	-1.593	0.8990	-1.011	73.633	-2.983	4.2510	0.0235
	≠	SSNPT	8.9765	2.270	0.8802	1.101	70.856	0.900	4.3214	-1.680
	0	HSDT	8.9197	2.888	0.8738	1.820	70.230	1.775	4.3342	-1.981
	0	FSDT	8.0057	12.83	0.8136	8.584	63.033	11.84	4.4226	-4.061
	0	CPT	8.0057	12.83	0.5097	42.73	63.033	11.84	4.4226	-4.061
	≠0	Elasticity	9.1850	0.000	0.8900	0.000	71.500	0.000	4.2500	0.000

FOSNDT: Present, SSNPT: Sayyad and Ghugal (2016), HSDT: Reddy (1984), FSDT: Mindlin (1951), CPT: Kirchhoff (1850), Elasticity: Pagano (1969)

Table 4*. Comparison of In-Plane Displacement, Transverse Displacement, In-Plane Normal Stress and Transverse Shear Stress for Three-Layer (0^0/Core/90^0) Symmetric Laminated Composite Plate Subjected to Sinusoidal Load under Cylindrical Bending*

a/h	ε_z	Model	$\bar{u}^{max}$	$\bar{w}^{max}$	$\bar{\sigma}_x^{max}$	$\bar{\tau}_{xz}^{max}$
4	≠0	FOSNDT	1.9096	8.6150	28.8295	1.4005
	≠0	SSNPT	1.8901	8.4532	28.9670	1.3841
	0	HSDT	1.9081	8.5369	28.6061	1.3855
	0	FSDT	1.3295	5.4694	19.9320	1.4089
	0	CPT	1.3295	1.3225	19.9320	1.4089
10	≠0	FOSNDT	22.203	2.4914	133.100	3.5242
	≠0	SSNPT	22.092	2.4739	133.754	3.5122
	0	HSDT	22.235	2.4889	133.340	3.5128
	0	FSDT	20.773	1.9860	124.575	3.5223
	0	CPT	20.773	1.3225	124.575	3.5223
100	≠0	FOSNDT	20781.0	1.3337	12433.0	35.285
	≠0	SSNPT	20680.2	1.3272	12477.5	35.220
	0	HSDT	20.788.4	1.3342	12466.4	35.222
	0	FSDT	20773.2	1.3291	12457.3	35.221
	0	CPT	20773.2	1.3225	12457.3	35.221

FOSNDT: Present, SSNPT: Sayyad and Ghugal (2016), HSDT: Reddy (1984), FSDT: Mindlin (1951), CPT: Kirchhoff (1850)

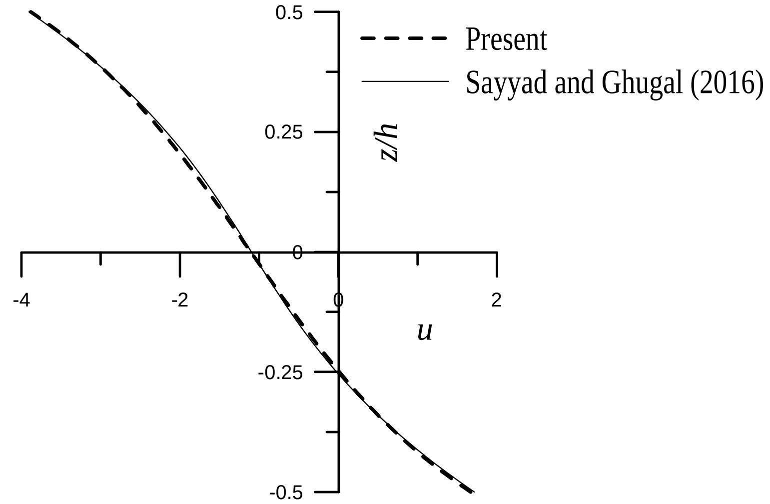

Figure 3: *Through thickness variation of in-plane displacement ($\overline{u}$) at (x=0, z) for two-layer ($0^0/90^0$) antisymmetric laminated composite plate subjected to sinusoidal load. (a/h=4)*

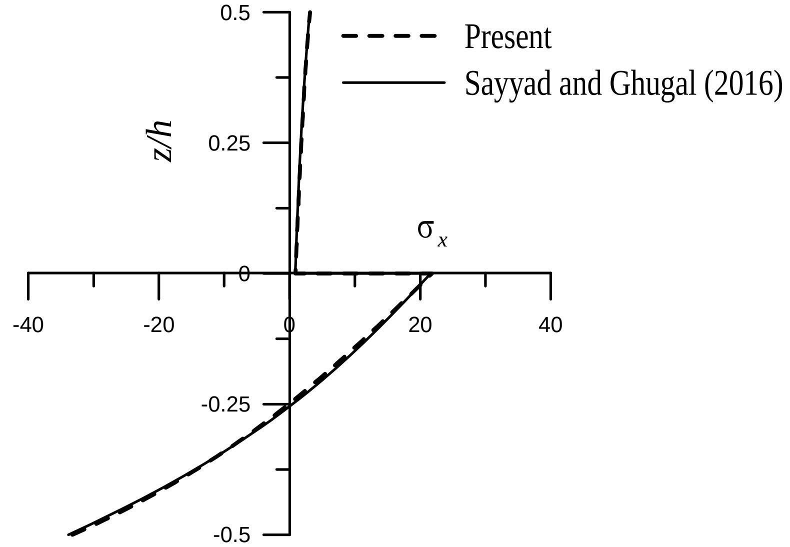

Figure 4: *Through thickness variation of in-plane normal stress ($\overline{\sigma}_x$) at (x=a/2, z) for two-layer ($0^0/90^0$) antisymmetric laminated composite plate subjected to sinusoidal load (a/h=4)*

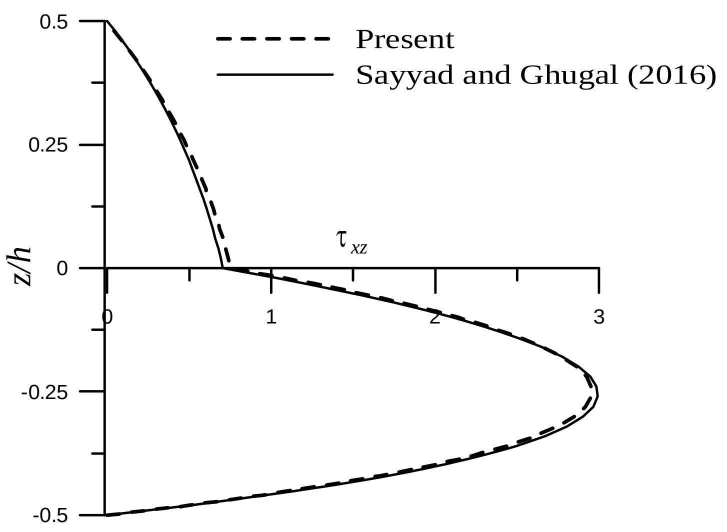

Figure 5: *Through thickness variation of transverse shear stress ($\overline{\tau}_{xz}$) at (x=0, z) for two-layer ($0^0/90^0$) antisymmetric laminated composite plate subjected to sinusoidal load (a/h=4)*

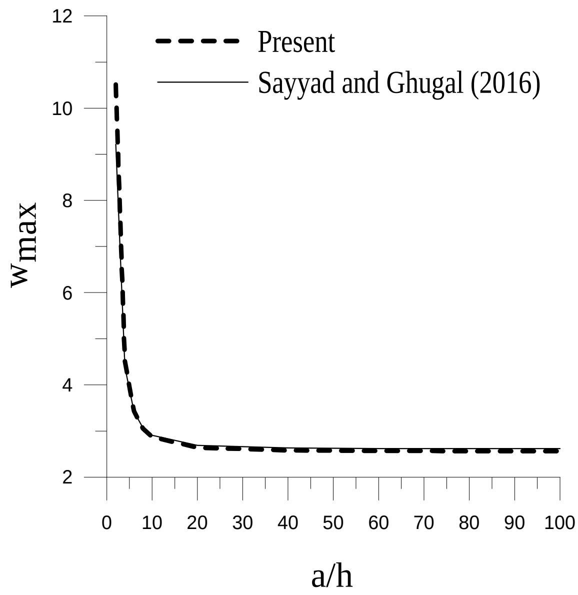

Figure 6: *Variation of transverse displacement ($\overline{w}$) with respect to aspect ratio for two-layer ($0^0/90^0$) antisymmetric laminated composite plate subjected to sinusoidal load.*

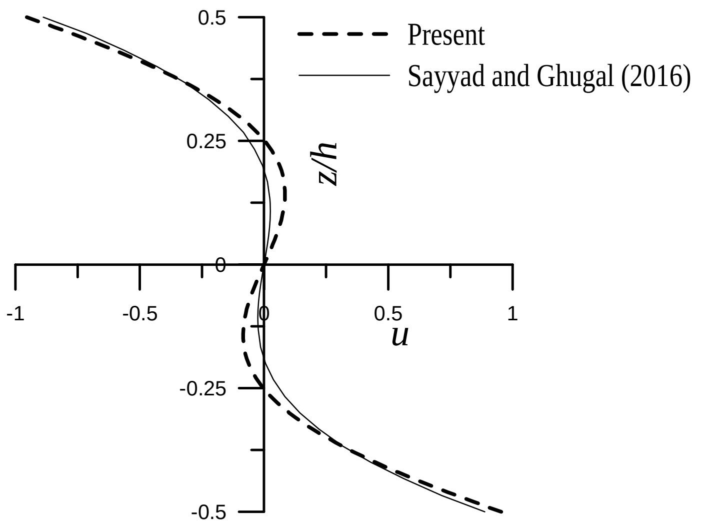

Figure 7: *Through thickness variation of in-plane displacement ($\overline{u}$) at (x=0, z) for three-layer ($0^0/90^0/0^0$) symmetric laminated composite plate subjected to sinusoidal load. (a/h=4)*

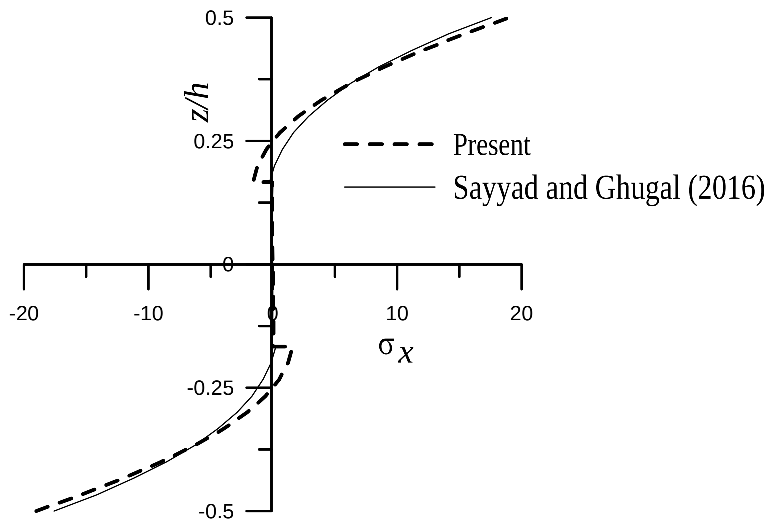

***Figure 8**: Through thickness variation of in-plane normal stress ($\overline{\sigma}_x$) at (x=a/2, z) for three-layer ($0^0/90^0/0^0$) symmetric laminated composite plate subjected to sinusoidal load (a/h=4)*

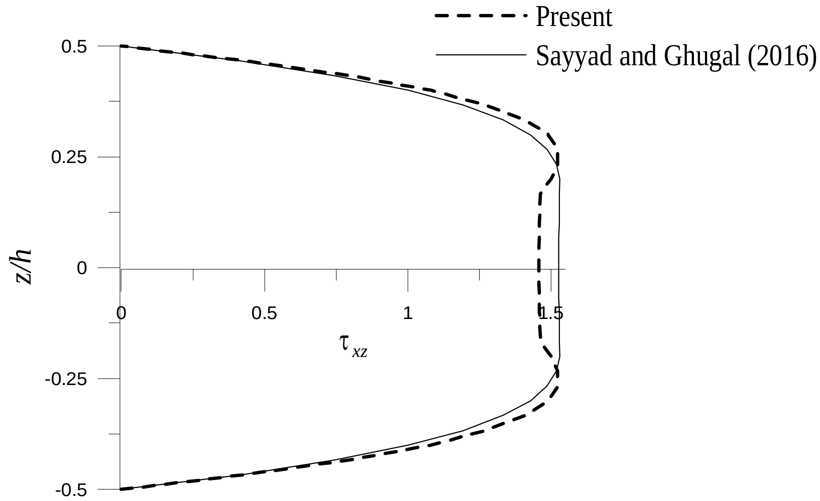

Figure 9: *Through thickness variation of transverse shear stress ($\bar{\tau}_{xz}$) at (x=0, z) for three-layer ($0^0/90^0/0^0$) symmetric laminated composite plate subjected to sinusoidal load. (a/h=4)*

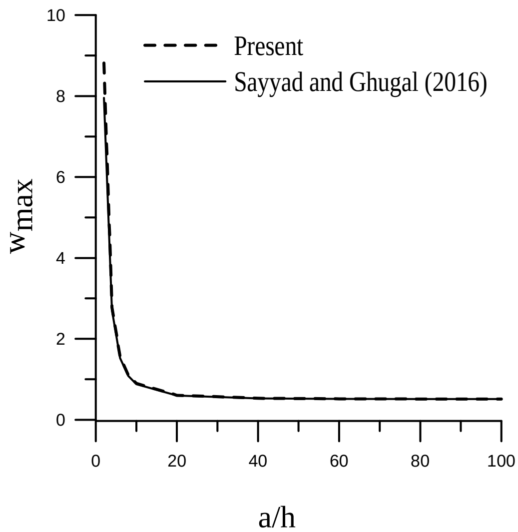

Figure 10: *Variation of transverse displacement ($\bar{w}$) with respect to aspect ratio for three-layer ($0^0/90^0/0^0$) symmetric laminated composite plate subjected to sinusoidal load*

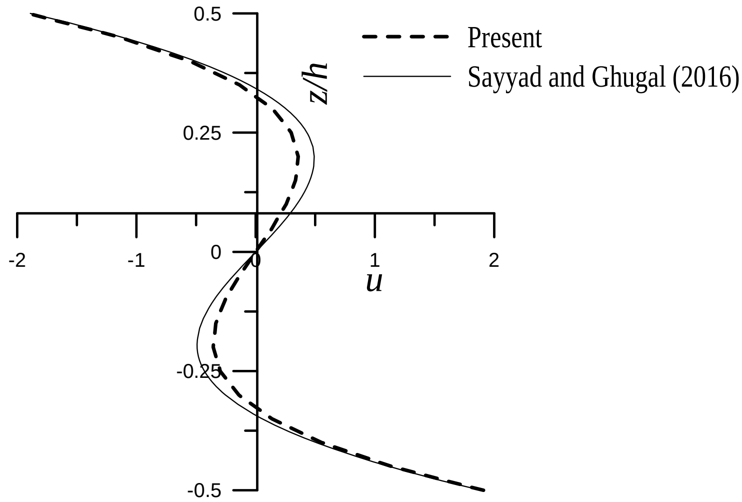

***Figure 11**: Through thickness variation of in-plane displacement ($\bar{u}$) at (x=0, z) for three-layer (0^0/core/0^0) symmetric sandwich plate subjected to sinusoidal load. (a/h=4)*

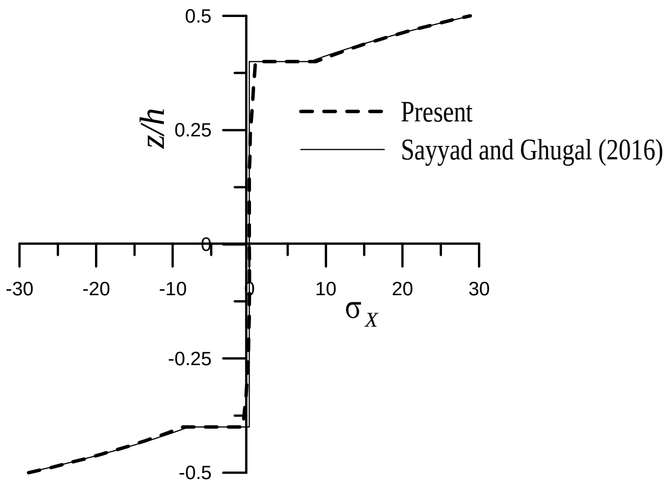

Figure 12: *Through thickness variation of in-plane normal stress ($\overline{\sigma}_x$) at (x=a/2, z) for three- layer (0^0/core/0^0) symmetric sandwich plate subjected to sinusoidal load. (a/h=4)*

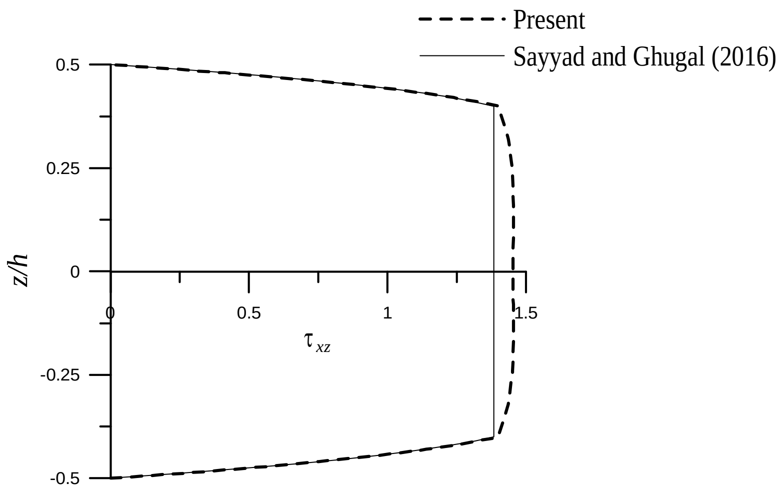

Figure 13: *Through thickness variation of transverse shear stress ($\overline{\tau}_{xz}$) at (x=0, z) for three-layer (0^0/core/0^0) symmetric sandwich plate subjected to sinusoidal load. (a/h=4)*

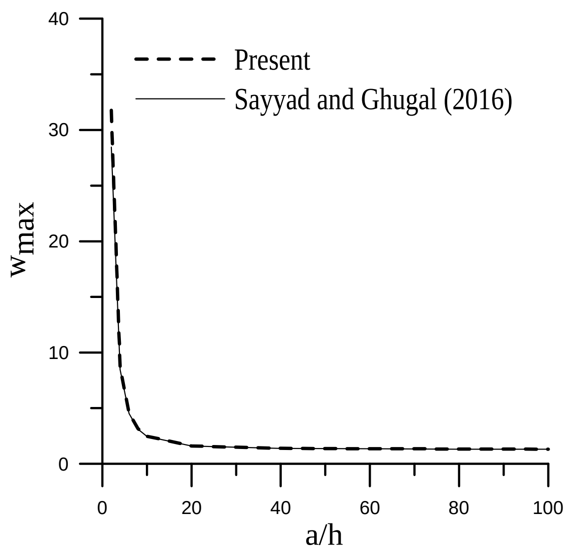

Figure 14*: Variation of transverse displacement ($\overline{w}$) with respect to aspect ratio for three-layer (0^0/core/90^0) symmetric sandwich plate subjected to sinusoidal load.*

4.0 CONCLUSIONS

A new fifth-order shear and normal deformation theory for the cylindrical bending of laminated composite and sandwich plates have been developed in this paper. To account for the effect of transverse shear deformation, in-plane displacement uses polynomial shape function expanded up to fifth-order in-terms of the thickness coordinate. The present theory involves six-degrees-of-freedom. The theory satisfies traction free boundary conditions at top and bottom surfaces of the plate and does not required the shear correction factor. For simplicity, this theory is applied for the analysis of laminated composite and sandwich plates deformed in cylindrical bending. Non-dimensional displacements and stresses obtained using the present theory are compared with existing exact elasticity solutions and lower and higher-order theories. From the comparison of numerical results, it is concluded that the present theory is in good agreement with exact elasticity solution of Pagano and shows considerable improvement in the numerical results obtained by using higher-order shear deformation theory of Reddy. This validate that the effect of transverse shear and normal deformations both plays important role in the analysis of laminated composite structures.

References

Carrera, E. (2005). Transverse normal strain effects on thermal stress analysis of homogeneous and layered plates. AIAA Journal 43(10): 2232-2242.

Carrera, E. and Zappino, E. (2016). CUF based variable kinematic models for free-vibration analysis of aircraft structures. AIAA Journal 54(1): 280-292.

Carrera, E., Giunta, G., and Petrolo, M. (2011). Beam Structures: Classical and Advanced Theories, John Wiley & Sons Ltd U.K.

Chakrabarti, A., and Sheikh, A. H. (2005). Analysis of laminated sandwich plates based on interlaminar shear stress continuous plate theory. ASCE Journal ofEngineering Mechanics 131(4): 377-384.

Fares, M. E., and Elmarghany, M. (2008). A refined zigzag nonlinear first order shear deformation theory of composite laminated plates. Composite Structures 82:71-83.

Ferreira, A. J. M., Roque, C. M. C., Carrera, E. and Cinera, M. (2011). Two higher order zig-zag theories for the accurate analysis of bending, vibration and buckling response of laminated plates by radial basis function collocation and a unified formulation. Journal of Composite Materials 45(24): 2523-2536.

Ghugal, Y. M. and Sayyad, A. S. (2011). Free vibration of thick isotropic plates using trigonometric shear deformation theory. Journal of Solid Mechanics 3: 172–182.

Kant, T., and Kommineni, J. R. (1994). Nonlinear analysis of angle ply composite and sandwich laminates. ASCEJournal of Aerospace Engineering 7(3): 342-352.

Kant, T., and Shiyekar, S. M. (2008). Cylindrical bending of piezoelectric laminates with a higher order shear and normal deformation theory. Computers and Structures 86: 1594-1603.

Kant, T., and Swaminathan, K. (2000). Analytical solutions for the static analysis of laminated composite and sandwich plates based on a higher order refined theory. Composite Structures 56:329-344.

Kapuria, S., Dumir, P.C., and Jain, N. K. (2004). Assessment of zigzag theory for static loading, buckling, free and forced response of composite and sandwich beams. Composite Structures 64: 317-327.

Kirchhoff, G.R., (1850). Uber das gleichgewicht und die bewegung einer elastischen Scheibe. Journal für die Reine und Angewandte Mathematik (Crelle's Journal) 40: 51-88.

Krishna Murty, A. V. (1984). Toward a consistent beam theory. AIAA Journal 22 (6): 811-816.

Mindlin, R.D. (1951). Influence of rotary inertia and shear on flexural motions of isotropic, elastic plates. ASME Journal of Applied Mechanics18: 31-38.

Pagani, A., de Miguel, A. G., Petrolo, M. and Carrera, E. (2016). Analysis of laminated beams via unified formulation and Legendre polynomial expansions. Composite Structures 156: 78-92.

Pagano, N. J. (1969). Exact solution for composite laminates in cylindrical bending. Journal of Composite Materials 3: 398-411.

Pagano, N. J. (1970a). Exact solutions for bidirectional composites and sandwich plates. Journal of Composite Materials 4: 20–34.

Pagano, N. J. (1970b). Influence of shear coupling in cylindrical bending of anisotropic laminates. Journal of Composite Materials 4: 330-343.

Reddy, J. N. (1984). A simple higher order theory for laminated composite plates. ASMEJournal of Applied Mechanics 51:745-752.

Sarangan S., and Singh, B. N. (2016). Higher order closed form solution for the analysis of laminated composite and sandwich plates based on new shear deformation theories. Composite Structures 138: 391-403.

Sayyad, A. S., and Ghugal, Y. M. (2015a). On the free vibration analysis of laminated composite and sandwich plates: A review of recent literature with some numerical results. Composite Structures 29: 177-201.

Sayyad, A. S., and Ghugal, Y. M. (2015b). A *n*th-order shear deformation theory for composite laminates in cylindrical bending. Curved and Layered Structures 2: 290-300.

Sayyad, A. S., and Ghugal, Y. M. (2016). Cylindrical bending of multilayered composite laminates and sandwiches. Advances in Aircraft and Spacecraft Sciences 3(2): 113-148.

Sayyad, A. S., and Ghugal, Y. M. (2017a). Bending, buckling and free vibration of laminated composite and sandwich beams: A critical review of literature. Composite Structures 171: 486-504.

Sayyad, A. S., and Ghugal, Y. M. (2017b). A unified shear deformation theory for the bending of isotropic, functionally graded, laminated and sandwich beams and plates. International Journal of Applied Mechanics 9(1):1-36.

Shu, X.P., and Soldatos, K. P. (2000). Cylindrical bending of angle-ply laminates subjected to different sets of edge boundary conditions. International Journal of Solids and Structures 37: 4289-4307.

Soldatos, K. P., and Watson, P. (1997). A method for improving the stress analysis performance of one-and two-dimensional theories for laminated composites. Acta Mechanica 123(1):163-186.

Timoshenko, S., and Woinowsky-Krieger, S. (1959). Theory of plates and shells. McGraw Hill, New York.

Todhunter, I., and Pearson, K. (1960). A history of the theory of elasticity and of the strength of materials from Galileo Galilei (1564-1642) to Lord Kelvin (1824-1907). Vols. I, II and III, Dover Publications, Inc., New York.

Zhen, W., and Wanji, C. (2007). Study of global-local higher order theories for laminated composite plates. Composite Structures 79: 44-54.